

Journal of Mechanics of Materials and Structures

**A STUDY OF ELASTIC-PLASTIC DEFORMATION IN THE PLATE
WITH THE INCREMENTAL THEORY AND THE MESHLESS METHODS**

Malgorzata A. Jankowska and Jan Adam Kołodziej

Volume 11, No. 1

January 2016



A STUDY OF ELASTIC-PLASTIC DEFORMATION IN THE PLATE WITH THE INCREMENTAL THEORY AND THE MESHLESS METHODS

MALGORZATA A. JANKOWSKA AND JAN ADAM KOŁODZIEJ

The paper concerns an application of the successive-approximation iteration process together with the meshless methods, i.e., the method of fundamental solutions (MFS) and the method of particular solutions (MPS), for the analysis of strains and stresses in the plate with some kind of narrowing subjected to uniaxial tension. The elastoplastic boundary-value problem is based on the incremental theory of plasticity with the stress-strain relation given in the form proposed by Chakrabarty. In the iteration procedure a sequence of the successive distributions of the plastic strain increments corresponding to the appropriate increments of load is produced. A final set of the plastic strain increments is further used to obtain the total plastic strains. Furthermore, the solution of the elastoplastic boundary-value problem can be simultaneously taken into account when the stress state of the plate is required. Such approach is designated here to identify the regions of elastic and plastic behavior of the material.

1. Introduction

The most popular and commonly used method for solving the elastoplastic problems is the finite element method (FEM). There are many papers on this subject (see, e.g., [Berezhnoĭ and Paĭmushin 2011; Bilotta and Casciaro 2007; Cui et al. 2009; Liu et al. 2013; 2012]) as well as the available monographs (see, e.g., [Belytschko et al. 2000; Crisfield 1997; Kojić and Bathe 2005; Owen and Hinton 1980]). A numerical method that is much less employed for this class of problems is the boundary element method (BEM). Nevertheless, the number of publications on this topic is quite extensive and new ones are still emerging [Deng et al. 2011; Gao and Davies 2000; Ochiai 2011]. We can also distinguish a coupling of these two approaches in, e.g., [Boumaiza and Aour 2014; Dong and Bonnet 1998; Oysu and Fenner 2006]. Note that all these methods require some kind of mesh to be prepared, and hence they are called mesh methods. As an alternative approach for the mesh methods, the mesh-free methods have been developed in the last decades. The meshless methods have been also applied for solving some elastic-plastic problems [Boudaia et al. 2009; Dai et al. 2006; Liu et al. 2011; Pozo et al. 2009; Yeon and Youn 2005]. Nowadays, many different variants of these methods are studied. We have, e.g., the element-free Galerkin method, the meshless local Petrov–Galerkin method, the point interpolation method, the finite point method, the finite difference method with arbitrary irregular grids, and so forth [Liu 2003]. The method of fundamental solutions (MFS) and the method of particular solutions (MPS), subsequently used by the authors, are both the meshfree methods. The main idea of the MFS is that an approximate solution of

The work of Jankowska was supported by the Poznan University of Technology (Poland) through Grants No. 02/21/DSPB/3453 and 02/21/DSPB/3463. The work of Kołodziej was supported by Grant No. 2012/07/B/ST8/03449 founded by the Polish National Science Center (NCN).

Keywords: meshless methods, method of fundamental solutions, successive-approximation iteration process, elastic-plastic deformation, incremental theory.

a given problem is formulated as a linear combination of fundamental solutions related to a governing equation that is linear and homogeneous. Hence, if the appropriate fundamental solutions are known, we obtain an approximate solution that satisfies a governing differential equation and only boundary conditions are approximately met. On the other hand, the MPS can be applied for the boundary value problems with linear nonhomogeneous governing equations. As is described in detail in, e.g., [Chen et al. 2014], a solution of such a problem is a sum of so-called homogeneous solution and particular solution. Nowadays, there is a number of review papers that report on an application of the MFS for solving some elliptic problems [Fairweather and Karageorghis 1998], wave scattering problems [Fairweather et al. 2003] and inverse problems [Karageorghis et al. 2011]. On the other hand, there are still few papers that conduct a review on the usage of the MFS for solving nonlinear problems. An application of the method considered for nonlinear problems is quite popular in the area of fluid mechanics and there are many papers that take into account this issue. Namely, for a governing equation given in a form of Burgers' equation we have [Young et al. 2008], similarly as for the Navier–Stokes equation [Young et al. 2009] and for nonlinear water waves [Feng et al. 2013; Mollazadeh et al. 2011]. A solution of a boundary value problem governed by a nonlinear Poisson equation is presented in, e.g., [Balakrishnan and Ramachandran 1999; 2001; Balakrishnan et al. 2002; Burgess and Mahajerin 1987; Fallahi and Hosami 2011; Shanazari and Fallahi 2010; Tri et al. 2011; Tsai 2012; Wang and Qin. 2006; Wang et al. 2012]. Further, in [Chen 1995] the nonlinear thermal explosion problem by solving some nonlinear equation is taken into consideration. An application of the MFS for nonlinear functionally graded materials is given in [Li et al. 2014; Marin and Lesnic 2007; Wang and Qin. 2008; Wang et al. 2005], while the nonlinear heat conduction problems solved by the MFS are presented in [Karageorghis and Fairweather 1989; Karageorghis and Lesnic 2008]. Finally, nonlinear plate problems as well as an application of the MFS for nonlinear elasticity is reported in [Al-Gahtani 2012; Li and Zhu 2009; Uscilowska and Berendt 2013]. For the authors' best knowledge there are few papers such that the MFS with the MPS are applied to study elastic-plastic deformation. These articles deal with the torsion problem [Kołodziej et al. 2013] and the plane problem for the stress state of a plate subjected to uniaxial extension [Jankowska and Kołodziej 2015].

Subsequent considerations are directed forward further popularization and dissemination of the meshless methods for solving some nonlinear boundary-value problems with a special attention that is paid to elastoplastic problems. The authors based their research on the approach proposed in [Mendelson 1968]. It takes into account the incremental theory of plasticity together with the associated flow rule given by the Prandtl–Reuss relation and the von Mises yield criterion to formulate the appropriate elastoplastic plane stress problem (see Section 2). The appropriate boundary conditions concern a problem of uniaxial tension of a plate with a narrowing located in the middle of it (see also [Jankowska and Kołodziej 2014; Jankowska and Kołodziej 2013]). Then, for the nonlinear stress-strain relationship, we apply a model presented by Chakrabarty in [Chakrabarty 1987]. In Section 3 a new approach to the successive-approximation iteration process [Mendelson 1968] is proposed. It employs a combination of the meshless methods (the MFS-MPS) and the finite difference schemes (required for the approximation of values of partial derivatives present in the right-hand side function of the problem). In the appropriate algorithm, a sequence of the successive distributions of the plastic strain increments, corresponding to a given increment of load, is produced. A final set of the plastic strain increments can be used to obtain the total plastic strains. Then, the solution of the boundary-value problem let us determine the stress state of

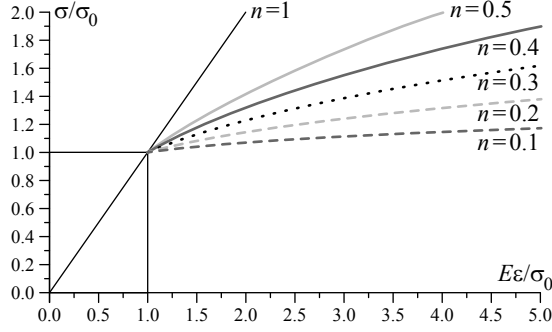


Figure 1. The stress-strain curve for the model proposed by Chakrabarty [1987] with selected values of n .

the plate. In Section 4, the optimal values of the method's parameters are proposed and the regions of the elastic and plastic behavior of the material are shown. The approach enables to compute the equivalent plastic strains and also related equivalent stresses in any point of the domain. It is due to the fact that the approximate solution is a linear combination of fundamental solutions and particular solutions, i.e., a continuous function with continuous derivatives. To conclude, some final remarks and further plans are summarized in Section 5.

2. Problem formulation

2.1. Assumptions about the elastic-plastic constitutive model and the complete stress-strain relations.

The consideration given in the paper concerns some plane elastoplastic problem formulated for a plate with a narrowing subjected to external loads related to the uniaxial stress σ_B . We assume that the material is homogenous, isotropic and strains hardens isotropically. The material properties such as the Young modulus E and the Poisson ratio ν are independent of the temperature and body forces are not considered. For the nonlinear stress-strain relationship we employ a model proposed by Chakrabarty [1987]. It is given by the equations

$$\sigma/\sigma_0 = \begin{cases} \varepsilon/\varepsilon_0, & \varepsilon/\varepsilon_0 \leq 1, \\ (\varepsilon/\varepsilon_0)^n, & \varepsilon/\varepsilon_0 \geq 1. \end{cases} \quad (1)$$

Note that the curve in the plastic range is expressed by a simple power law (see also Figure 1) with a dimensionless constant n such that its value is generally less than 0.5. The material is assumed to have a definite yield point for the stress σ_0 with the corresponding yield strain $\varepsilon_0 = \sigma_0/E$, where E is the Young modulus. Furthermore, the slope of the stress-strain curve changes discontinuously at the yield point (except for the case of $n = 1$).

The subsequent considerations are presented with the incremental theory of plasticity applied (see, e.g., [Mendelson 1968]). Hence, we assume some loading path to a given state of stress and the total plastic strain. The total loading path is divided into N increments of load. When the load is increased by a small amount, it produces additional plastic strain $\Delta\varepsilon_{ij}^P$. Following, e.g., [Mendelson 1968], the total strain ε_{ij} can be written as

$$\varepsilon_{ij} = \varepsilon_{ij}^e + \varepsilon_{ij}^P + \Delta\varepsilon_{ij}^P, \quad (2)$$

where ε_{ij}^e is the elastic component of the strain, ε_{ij}^p is the accumulated plastic strain up to (but not including) the current increment of load and $\Delta\varepsilon_{ij}^p$ is the increment of plastic strain due to the current increment of load. If we assume that the elastic strain tensor is given by the Hooke's law for isotropic material and the plastic strains have been computed for the first $k - 1$ increments of load, then the total strain at the end of the k -th increment of load can be given as follows:

$$\varepsilon_{ij} = \frac{1+\nu}{E}\sigma_{ij} - \frac{\nu}{E}\sigma_{ss}\delta_{ij} + \sum_{m=1}^{k-1}\Delta\varepsilon_{ij,m}^p + \Delta\varepsilon_{ij}^p. \quad (3)$$

In the above equation we know the sum and the problem is how to calculate the plastic strain increment $\Delta\varepsilon_{ij}^p$ (for the current, i.e., the k -th increment of load) and the corresponding stress. Hence, subsequently for the equation (3) we use the stress-strain relation (1), the associated flow rule given by the Prandtl–Reuss relation (4)₁ with the von Mises yield criterion (4)₂. The equivalent stress σ_{eq} , the equivalent plastic strain increment $\Delta\varepsilon_{ij}^p$ and the deviatoric component S_{ij} of the stress tensor are given by the equations

$$\Delta\varepsilon_{ij}^p = \frac{3}{2}\frac{\Delta\varepsilon_{\text{eq}}^p}{\sigma_{\text{eq}}}S_{ij}, \quad \sigma_{\text{eq}} = \sqrt{\frac{3}{2}S_{ij}S_{ij}}, \quad \Delta\varepsilon_{\text{eq}}^p = \sqrt{\frac{2}{3}\Delta\varepsilon_{ij}^p\Delta\varepsilon_{ij}^p}, \quad S_{ij} = \sigma_{ij} - \frac{1}{3}\sigma_{ss}\delta_{ij}. \quad (4)$$

2.2. Plane elastic-plastic boundary-value problem. Now we formulate the boundary-value problem describing the stress state of the plate that is subjected to uniaxial extension related to the stress σ_B . However, before that we expand the equations (3)–(4) with the assumption that the generalized plane stress problem is considered. We obtain the formulas for the components of the total strain (3) as

$$\varepsilon_{xx} = \varepsilon_{xx}^e + \varepsilon_{xx}^p + \Delta\varepsilon_{xx}^p, \quad \varepsilon_{yy} = \varepsilon_{yy}^e + \varepsilon_{yy}^p + \Delta\varepsilon_{yy}^p, \quad \varepsilon_{xy} = \varepsilon_{xy}^e + \varepsilon_{xy}^p + \Delta\varepsilon_{xy}^p, \quad (5)$$

where

$$\varepsilon_{xx}^e = \frac{1}{E}(\sigma_{xx} - \mu\sigma_{yy}), \quad \varepsilon_{yy}^e = \frac{1}{E}(\sigma_{yy} - \mu\sigma_{xx}), \quad \varepsilon_{xy}^e = \frac{1}{2G}\sigma_{xy}, \quad (6)$$

$$\varepsilon_{xx}^p = \sum_{m=1}^{k-1}\Delta\varepsilon_{xx,m}^p, \quad \varepsilon_{yy}^p = \sum_{m=1}^{k-1}\Delta\varepsilon_{yy,m}^p, \quad \varepsilon_{xy}^p = \sum_{m=1}^{k-1}\Delta\varepsilon_{xy,m}^p. \quad (7)$$

Then, the expanded formulas for the Prandtl–Reuss relations (4)₁ with the equivalent stress (4)₂ and the equivalent plastic strain increments (4)₃ are of the form (see also [Mendelson 1968])

$$\Delta\varepsilon_{xx}^p = \frac{1}{2}\frac{\Delta\varepsilon_{\text{eq}}^p}{\sigma_{\text{eq}}}(2\sigma_{xx} - \sigma_{yy}), \quad \Delta\varepsilon_{yy}^p = \frac{1}{2}\frac{\Delta\varepsilon_{\text{eq}}^p}{\sigma_{\text{eq}}}(2\sigma_{yy} - \sigma_{xx}), \quad \Delta\varepsilon_{xy}^p = \frac{3}{2}\frac{\Delta\varepsilon_{\text{eq}}^p}{\sigma_{\text{eq}}}\sigma_{xy}, \quad (8)$$

and

$$\sigma_{\text{eq}} = \sqrt{\sigma_{xx}^2 + \sigma_{yy}^2 - \sigma_{xx}\sigma_{yy} + 3\sigma_{xy}^2}, \quad \Delta\varepsilon_{\text{eq}}^p = \frac{2}{\sqrt{3}}\sqrt{(\Delta\varepsilon_{xx}^p)^2 + (\Delta\varepsilon_{yy}^p)^2 + \Delta\varepsilon_{xx}^p\Delta\varepsilon_{yy}^p + (\Delta\varepsilon_{xy}^p)^2}. \quad (9)$$

Subsequently, we take into consideration the boundary-value problem as proposed in [Mendelson 1968]. For its formulation the components of the total strain (5) with the relations (6)–(7) are substituted into the compatibility and equilibrium equations for the plane problems (see, e.g., [Mendelson 1968;

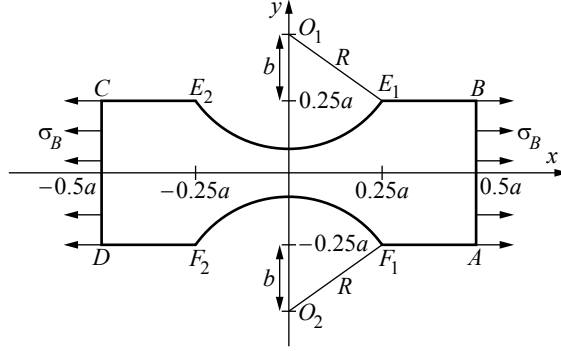


Figure 2. A plate with a narrowing subjected to uniaxial extension related to the stress σ_B (reprinted from [Jankowska and Kołodziej 2015] with permission from Elsevier).

[Timoshenko and Goodier 1951]). Then, with the Airy stress function $\psi = \psi(x, y)$ (see also [Timoshenko and Goodier 1951]) such that

$$\sigma_{xx} = \frac{\partial^2 \psi}{\partial y^2}(x, y), \quad \sigma_{yy} = \frac{\partial^2 \psi}{\partial x^2}(x, y), \quad \sigma_{xy} = -\frac{\partial^2 \psi}{\partial x \partial y}(x, y), \quad (10)$$

we obtain the governing equation of the problem considered

$$\nabla^4 \psi(x, y) = -(g(x, y) + \Delta g(x, y)), \quad (11)$$

where

$$g(x, y) = E \left(\frac{\partial^2 \varepsilon_{xx}^p}{\partial y^2} + \frac{\partial^2 \varepsilon_{yy}^p}{\partial x^2} - 2 \frac{\partial^2 \varepsilon_{xy}^p}{\partial x \partial y} \right), \quad (12)$$

$$\Delta g(x, y) = E \left(\frac{\partial^2 (\Delta \varepsilon_{xx}^p)}{\partial y^2} + \frac{\partial^2 (\Delta \varepsilon_{yy}^p)}{\partial x^2} - 2 \frac{\partial^2 (\Delta \varepsilon_{xy}^p)}{\partial x \partial y} \right).$$

In order to formulate the boundary conditions of the problem, we introduce the geometry of the plate (see Figure 2). It is characterized by the narrowing that occurs in the middle of it and is present along a half of its length. It is specified by the characteristic length a and the distance b such that the appropriate parts of the boundary, i.e., $E_1 E_2$, $F_1 F_2$, are arcs of circles with centers $O_1(0, a/4 + b)$, $O_2(0, -a/4 - b)$ and a radius $R = \sqrt{b^2 + a^2/16}$. The appropriate boundary conditions imposed according to the sides of the plate are given as

$$\Gamma_{AB} \text{ and } \Gamma_{DC} : \quad \psi_{yy} = \sigma_B, \quad \psi_{xy} = 0, \quad (13a)$$

$$\Gamma_{E_1 B}, \Gamma_{E_2 C} \text{ and } \Gamma_{F_1 A}, \Gamma_{F_2 D} : \quad \psi_{xx} = 0, \quad \psi_{xy} = 0, \quad (13b)$$

$$\Gamma_{E_1 E_2}, \Gamma_{F_1 F_2} : \quad \psi_{yy} n_x - \psi_{xy} n_y = 0, \quad \psi_{xx} n_y - \psi_{xy} n_x = 0, \quad (13c)$$

where n_x, n_y are components of a unit vector \mathbf{n} defined at a given point of the boundary, normal to the surface and directed outside of the plate.

Note that in the equations (13a)–(13c) and later in the paper, we use the abbreviated notation for partial derivatives, i.e., $\psi_{xx} = \partial^2 \psi / \partial x^2$, $\psi_{yy} = \partial^2 \psi / \partial y^2$ and $\psi_{xy} = \partial^2 \psi / \partial x \partial y$, respectively.

Subsequently, we solve the elastic-plastic boundary-value problem given in the nondimensional form. Hence, with new coordinates defined by

$$X = x/a, \quad Y = y/a, \quad \Psi = \psi/(a^2\sigma_0), \quad (14)$$

the governing equation (11) with (12) is of the form

$$\nabla^4\Psi = \tilde{b}(X, Y), \quad (15)$$

with the boundary conditions

$$\Gamma_{AB} \text{ and } \Gamma_{DC} : \quad \Psi_{YY} = \tilde{\sigma}_B, \quad \Psi_{XY} = 0, \quad (16a)$$

$$\Gamma_{E_1B}, \Gamma_{E_2C} \text{ and } \Gamma_{F_1A}, \Gamma_{F_2D} : \quad \Psi_{XX} = 0, \quad \Psi_{XY} = 0, \quad (16b)$$

$$\Gamma_{E_1E_2}, \Gamma_{F_1F_2} : \quad \Psi_{YY}n_x - \Psi_{XY}n_y = 0, \quad \Psi_{XX}n_y - \Psi_{XY}n_x = 0, \quad (16c)$$

where $\tilde{\sigma}_B = \sigma_B/\sigma_0$ and

$$\tilde{b}(X, Y) = -(\tilde{g}(X, Y) + \Delta\tilde{g}(X, Y)), \quad (17)$$

$$\tilde{g}(X, Y) = \left(\frac{\partial^2 \varepsilon_{XX}^p}{\partial Y^2} + \frac{\partial^2 \varepsilon_{YY}^p}{\partial X^2} - 2 \frac{\partial^2 \varepsilon_{XY}^p}{\partial X \partial Y} \right), \quad (18)$$

$$\Delta\tilde{g}(X, Y) = \left(\frac{\partial^2 (\Delta\varepsilon_{XX}^p)}{\partial Y^2} + \frac{\partial^2 (\Delta\varepsilon_{YY}^p)}{\partial X^2} - 2 \frac{\partial^2 (\Delta\varepsilon_{XY}^p)}{\partial X \partial Y} \right). \quad (19)$$

The dimensionless plastic strains $\varepsilon_{XX}^p = \varepsilon_{xx}^p/\varepsilon_0$, $\varepsilon_{YY}^p = \varepsilon_{yy}^p/\varepsilon_0$ and $\varepsilon_{XY}^p = \varepsilon_{xy}^p/\varepsilon_0$, present in (18), are given by the formulas

$$\varepsilon_{XX}^p = \sum_{m=1}^{k-1} \Delta\varepsilon_{XX,m}^p, \quad \varepsilon_{YY}^p = \sum_{m=1}^{k-1} \Delta\varepsilon_{YY,m}^p, \quad \varepsilon_{XY}^p = \sum_{m=1}^{k-1} \Delta\varepsilon_{XY,m}^p, \quad (20)$$

where the dimensionless increments of plastic strains used in (19)–(20) are defined as $\Delta\varepsilon_{XX}^p = \Delta\varepsilon_{xx}^p/\varepsilon_0$, $\Delta\varepsilon_{YY}^p = \Delta\varepsilon_{yy}^p/\varepsilon_0$ and $\Delta\varepsilon_{XY}^p = \Delta\varepsilon_{xy}^p/\varepsilon_0$, respectively. Further, with the dimensionless Airy stress function $\Psi = \Psi(X, Y)$ applied, the dimensionless total strains and the elastic strains, are of the form

$$\varepsilon_{XX} = \varepsilon_{XX}^e + \varepsilon_{XX}^p + \Delta\varepsilon_{XX}^p, \quad \varepsilon_{YY} = \varepsilon_{YY}^e + \varepsilon_{YY}^p + \Delta\varepsilon_{YY}^p, \quad \varepsilon_{XY} = \varepsilon_{XY}^e + \varepsilon_{XY}^p + \Delta\varepsilon_{XY}^p, \quad (21)$$

$$\varepsilon_{XX}^e = \Psi_{YY} - \mu\Psi_{XX}, \quad \varepsilon_{YY}^e = \Psi_{XX} - \mu\Psi_{YY}, \quad \varepsilon_{XY}^e = -(1 + \mu)\Psi_{XY}, \quad (22)$$

where $\varepsilon_{XX} = \varepsilon_{xx}/\varepsilon_0$, $\varepsilon_{YY} = \varepsilon_{yy}/\varepsilon_0$, $\varepsilon_{XY} = \varepsilon_{xy}/\varepsilon_0$, $\varepsilon_{XX}^e = \varepsilon_{xx}^e/\varepsilon_0$, $\varepsilon_{YY}^e = \varepsilon_{yy}^e/\varepsilon_0$, $\varepsilon_{XY}^e = \varepsilon_{xy}^e/\varepsilon_0$.

Note that for the algorithm proposed in Section 3 that is designed for solving the boundary value equation (15)–(16) with (17)–(19), the dimensionless Prandtl–Reuss relations are also required. Hence, from the formula (8) we obtain

$$\Delta\varepsilon_{XX}^p = \frac{1}{2} \frac{\Delta\tilde{\varepsilon}_{\text{eq}}^p}{\tilde{\sigma}_{\text{eq}}} (2\sigma_{XX} - \sigma_{YY}), \quad \Delta\varepsilon_{YY}^p = \frac{1}{2} \frac{\Delta\tilde{\varepsilon}_{\text{eq}}^p}{\tilde{\sigma}_{\text{eq}}} (2\sigma_{YY} - \sigma_{XX}), \quad \Delta\varepsilon_{XY}^p = \frac{3}{2} \frac{\Delta\tilde{\varepsilon}_{\text{eq}}^p}{\tilde{\sigma}_{\text{eq}}} \sigma_{XY}, \quad (23)$$

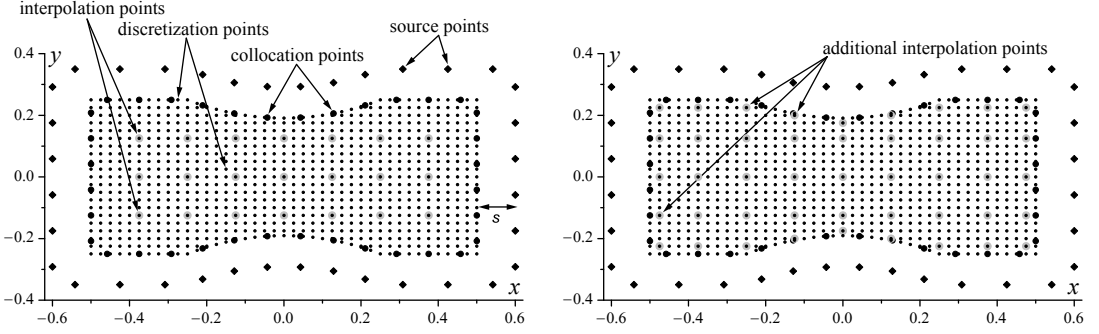


Figure 3. The distribution of the source, collocation, interpolation and discretization points.

where the dimensionless equivalent stress $\tilde{\sigma}_{\text{eq}} = \sigma_{\text{eq}}/\sigma_0$ and the dimensionless equivalent plastic strain increments $\Delta\tilde{\varepsilon}_{\text{eq}}^p$ are of the form

$$\tilde{\sigma}_{\text{eq}} = \sqrt{\sigma_{XX}^2 + \sigma_{YY}^2 - \sigma_{XX}\sigma_{YY} + 3\sigma_{XY}^2}, \quad (24)$$

$$\Delta\tilde{\varepsilon}_{\text{eq}}^p = \frac{2}{\sqrt{3}} \sqrt{(\Delta\varepsilon_{XX}^p)^2 + (\Delta\varepsilon_{YY}^p)^2 + \Delta\varepsilon_{XX}^p \Delta\varepsilon_{YY}^p + (\Delta\varepsilon_{XY}^p)^2}. \quad (25)$$

The dimensionless stress components used in (24) are defined as $\sigma_{XX} = \sigma_{xx}/\sigma_0$, $\sigma_{YY} = \sigma_{yy}/\sigma_0$, $\sigma_{XY} = \sigma_{xy}/\sigma_0$.

3. The successive-approximation iteration process and the meshless methods

Subsequently, we propose two algorithms that concern the solution of the boundary-value equation (15)–(16) with (17)–(19). The first one deals with a case when the whole region of the plate corresponds to the elastic behavior of the material. We propose the iteration process that proceeds until (for a given increment of load) the first points such that the plastic behavior of the material occurs. After that we can start the other two nested iteration processes described in detail in the second algorithm. The procedure proposed there let us determine the distribution of the plastic strain increments corresponding to a given conditions of loading. Moreover, the elastic and plastic strains and the stress state at each point of the plate can be also computed.

Note that both algorithms make use of the meshless methods (in each iteration step), i.e., the method of fundamental solutions and the method of particular solutions that is applied only in the Algorithm 2. Due to this reason we first generate some sets of points [Chen et al. 2014] that are required for the meshless methods (see also Figure 3, left). We denote by N_s the number of source points (X_{si}, Y_{si}) , $i = 1, 2, \dots, N_s$, that are located outside of the problem domain in a distance s from the boundary. For the numerical experiments they are uniformly distributed on a fictitious boundary similar to the physical one. We also choose the total number N_c of collocation points, (X_i, Y_i) , $i = 1, 2, \dots, N_c$. These points should be located as uniform as possible on the physical domain. Then, for the interpolation procedure of the right-hand side function (17), we select N_i interpolation points, (X_i, Y_i) , $i = 1, 2, \dots, N_i$, that are located inside of the computational domain. They used to be uniformly distributed similarly as the source and collocation points.

Special requirements of the subsequent algorithms make it essential to choose another set of uniformly distributed points, so-called, discretization points, (X_i, Y_i) , $i = 1, 2, \dots, Nd$. This set of points includes all the interpolation points together with some appropriate points located on the boundary (see Figure 3, left). The discretization points are further used for computation of values of partial derivatives present in (18)–(19) at the interpolation points. Note that the distances between two neighboring interpolation points does not have to be very small for the MPS. In fact the number of these points should not be also too large (because it can lead to an ill-conditioned matrix of coefficients further used in the MPS). On the other hand, the accuracy of a finite difference approximation increases when the distance between the points involved in a finite difference formula becomes small enough. Hence, we introduce the number iMd of additional intermediate discretization points that are located between each two interpolation points (see Figure 3, left). All these discretization points are involved in the finite difference approximation. Note that we also increase a number of the interpolation points in such a way that we add to the set considered some selected discretization points located near the boundary (see Figure 3, right). This approach is essential due to the fact that the material starts exhibiting the plastic behavior on the boundary and inside the plate in the neighborhood of the narrowing.

Now, with the assumptions and notations introduced above, the computational procedure can be formulated in the following way.

Algorithm 1 (elastic case). *Assumptions and preliminary steps.* We start from the assumption that the whole region of the plate corresponds to the elastic behavior of the material. Hence, for each iteration step we take $\tilde{b}(X, Y) \equiv 0$ in the governing equation (15). Then, we choose some loading path to a given state of stress, i.e., we take $m = 1, 2, \dots, k_p$ that corresponds to related values of stress $\tilde{\sigma}_B = \tilde{\sigma}_{B1}, \tilde{\sigma}_{B2}, \dots, \tilde{\sigma}_{Bk_p}$, respectively. The iteration step k_p is the last one performed during the algorithm's execution. For $m = k_p$ the material starts exhibiting the plastic behavior.

Step 1. Take $m = 1$ ($\tilde{\sigma}_B = \tilde{\sigma}_{B1}$).

Step 2. For a given value of m ($\tilde{\sigma}_{Bm}$), compute the approximate solution of the boundary value equation (15)–(16) using the MFS. We obtain

$$\Psi(X, Y) \approx \sum_{i=1}^{Ns} c_i \phi_{1i}(X, Y) + \sum_{i=1}^{Ns} d_i \phi_{2i}(X, Y), \quad (26)$$

where the functions $\phi_1 = \phi_1(X, Y)$, $\phi_2 = \phi_2(X, Y)$ are the fundamental solutions related to the homogeneous biharmonic equation $\nabla^4 \Psi = 0$. We have

$$\phi_{1i} = \phi_{1i}(X, Y) = \ln r_i, \quad \phi_{2i} = \phi_{2i}(X, Y) = r_i^2 \ln r_i, \quad r_i = \sqrt{(X - X_{si})^2 + (Y - Y_{si})^2}. \quad (27)$$

Unknown values of the coefficients c_i, d_i , $i = 1, 2, \dots, Ns$, in (26), can be found, if we solve a linear system of equations (28) obtained by collocating the boundary conditions. We get

$$G_{1l}(\Psi(X_j, Y_j)) = g_{1l}(X_j, Y_j), \quad G_{2l}(\Psi(X_j, Y_j)) = g_{2l}(X_j, Y_j), \quad (28)$$

for $l = 1, 2, \dots, Nl$, $j = 1, 2, \dots, Nc(l)$, where Ψ is of the form (26), G_{1l}, G_{2l} are the differential operators acting on Ψ , $g_{1l} = g_{1l}(X, Y)$, $g_{2l} = g_{2l}(X, Y)$ are given functions, Nl denotes the number of characteristic parts of the boundary and $Nc(l)$ denotes the number of collocation points located on a given part l of the boundary.

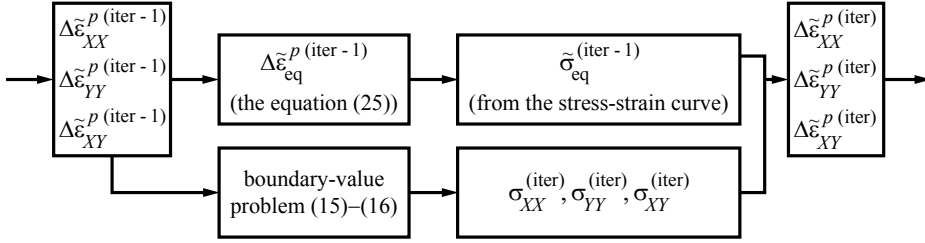


Figure 4. The block diagram [Mendelson 1968] that shows how to compute successive approximations of the plastic strain increments.

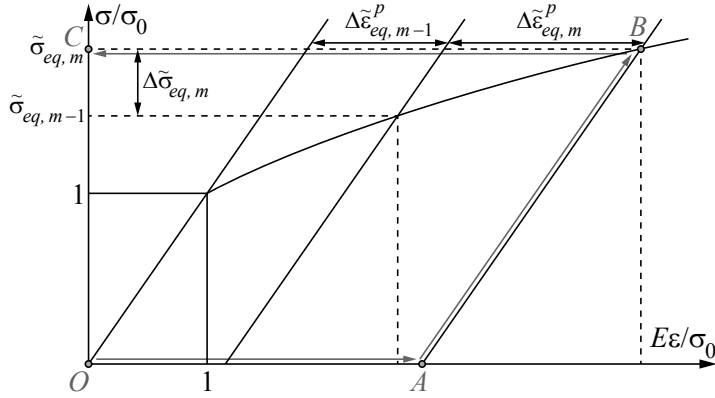


Figure 5. The stress-strain curve with the path $OABC$ [Mendelson 1968] that allows to obtain the equivalent stress $\tilde{\sigma}_{eq}$ from the equivalent plastic strain increment $\Delta \tilde{\varepsilon}_{eq}^p$.

Step 3. Compute the equivalent stress $\tilde{\sigma}_{eq,m}$ (the equation (24)) at each discretization point. Then, check if there exist one or more interpolation points such that $\tilde{\sigma}_{eq,m} > 1$. If so, then finish the execution of the Algorithm 1 and start the Algorithm 2. Else, take $m = m + 1$ ($\tilde{\sigma}_B = \tilde{\sigma}_{Bm}$), go back to Step 2 and continue the iteration process.

Algorithm 2 (elastic-plastic case). *Assumptions and preliminary steps.* On the basis of the results obtained with the Algorithm 1, the elastic-plastic behavior of the material is now considered. Hence, the right-hand side function in the governing equation (15) is no longer equal to zero. The Algorithm 2 consists of two nested iteration processes. In the case of the main iteration process we continue the loading path started by the Algorithm 1, i.e., we take $m = k_p, k_p + 1, \dots$, that corresponds to the stress $\tilde{\sigma}_B = \tilde{\sigma}_{Bk_p}, \tilde{\sigma}_{Bk_p+1}, \dots$, respectively. Note that since for the last iteration step k_p in the Algorithm 1 the elastic-plastic behavior of the material has been detected, then we repeat computations taking $m = k_p$ ($\tilde{\sigma}_B = \tilde{\sigma}_{Bk_p}$) and some initial distribution for the unknown plastic strain increments (further referred by $\text{iter} = 0$). Generally, for a given stress $\tilde{\sigma}_{Bm}$, we start the internal iteration process, taking $\text{iter} = 1, 2, \dots$. We compute successive approximations $\Delta \varepsilon_{XX}^{p(\text{iter})}, \Delta \varepsilon_{YY}^{p(\text{iter})}, \Delta \varepsilon_{XY}^{p(\text{iter})}$ for the plastic strain increments until a desired accuracy is achieved.

Main iteration process:

Step 1-1. Take $m = k_p$ ($\tilde{\sigma}_B = \tilde{\sigma}_{Bk_p}$).

Step 1-2. For a given value of m ($\tilde{\sigma}_{Bm}$), perform some preliminary steps, before the internal iteration process starts. An initial distribution of plastic strain increments is denoted as $\text{iter} = 0$.

If $m = k_p$, then

- (a) take $\varepsilon_{XX}^p = \varepsilon_{YY}^p = \varepsilon_{XY}^p = 0$ and $\tilde{g}(X_i, Y_i) = 0$, $i = 1, 2, \dots, Ni$;
- (b) choose some initial distribution for the plastic strain increments $\Delta\varepsilon_{XX}^{p(0)}$, $\Delta\varepsilon_{YY}^{p(0)}$, $\Delta\varepsilon_{XY}^{p(0)}$ for all discretization points such that $\tilde{\sigma}_{\text{eq},k_p} > 1$ (the [Algorithm 1](#)); for the remaining discretization points, take $\Delta\varepsilon_{XX}^{p(0)} = \Delta\varepsilon_{YY}^{p(0)} = \Delta\varepsilon_{XY}^{p(0)} = 0$.

Else, if $m > k_p$, then

- (a) use a final distribution of the plastic strain increments obtained for the stress $\tilde{\sigma}_{Bm-1}$ to compute current values of ε_{XX}^p , ε_{YY}^p , ε_{XY}^p (the equation (20)) for all interpolation points such that $\tilde{\sigma}_{\text{eq},m-1} > 1$; otherwise, take $\varepsilon_{XX}^p = \varepsilon_{YY}^p = \varepsilon_{XY}^p = 0$;
- (b) compute current values of the function $\tilde{g}(X_i, Y_i)$ (the equation (18)) at all interpolation points such that $\tilde{\sigma}_{\text{eq},m-1} > 1$ (see also the remarks on the finite difference (FD) approximation of the partial derivatives given below); otherwise, take $\tilde{g}(X_i, Y_i) = 0$;
- (c) choose some initial distribution for the plastic strain increments $\Delta\varepsilon_{XX}^{p(0)}$, $\Delta\varepsilon_{YY}^{p(0)}$, $\Delta\varepsilon_{XY}^{p(0)}$ for all discretization points such that $\tilde{\sigma}_{\text{eq},m-1} > 1$; otherwise, take $\Delta\varepsilon_{XX}^{p(0)} = \Delta\varepsilon_{YY}^{p(0)} = \Delta\varepsilon_{XY}^{p(0)} = 0$.

End If

Internal iteration process:

Step 2-1. Take $\text{iter} = 1$.

Step 2-2. Based on a given distribution of the plastic strain increments $\Delta\varepsilon_{XX}^{p(\text{iter}-1)}$, $\Delta\varepsilon_{YY}^{p(\text{iter}-1)}$, $\Delta\varepsilon_{XY}^{p(\text{iter}-1)}$ compute values of the function $\Delta\tilde{g}^{(\text{iter}-1)}(X_i, Y_i)$, $i = 1, 2, \dots, Ni$ (the equation (19); see also the remarks on the FD approximation of the partial derivatives).

Step 2-3. Compute values of the right-hand side function of the governing equation (15), i.e., $\tilde{b}^{(\text{iter}-1)}(X_i, Y_i)$, $i = 1, 2, \dots, Ni$ (the equation (17)).

Step 2-4. Compute the approximate solution of the inhomogeneous boundary value equation (15)–(16) using the MPS together with the MFS (see, e.g., [\[Chen et al. 2014\]](#)).

We represent the solution in a decomposed form as a sum of a particular solution $\Psi_p^{(\text{iter})}(X, Y)$ (see [Step 2-4-1](#)) and a general solution $\Psi_h^{(\text{iter})}(X, Y)$ (see [Step 2-4-2](#)), i.e.,

$$\Psi^{(\text{iter})}(X, Y) = \Psi_h^{(\text{iter})}(X, Y) + \Psi_p^{(\text{iter})}(X, Y). \quad (29)$$

Step 2-4-1. Compute the particular solution.

The particular solution satisfies the governing equation (15) in the domain, although it does not necessarily satisfy the boundary conditions. We can obtain the approximate particular solution if we interpolate the right-hand side function given in (15) at the interpolation points using radial basis functions (RBFs) φ_k and some polynomial functions p_j (for details see, e.g., [\[Chen et al. 2014; Jankowska and Kołodziej 2015\]](#)). Note that we take the multiquadric (MQ) as RBFs. We have

$$\varphi_k = \sqrt{(X - X_k)^2 + (Y - Y_k)^2 + c^2}, \quad (30)$$

where c is a shape parameter. Hence, we obtain

$$\tilde{b}^{(\text{iter}-1)}(X, Y) \approx \sum_{k=1}^{Ni} \alpha_k \varphi_k(X, Y) + \sum_{j=1}^L \beta_j p_j(X, Y), \quad (31)$$

where L , $0 \leq L \leq 6$, denotes the number of polynomials $p_j = p_j(X, Y)$ in (31). Note that α_k , β_j in (31) are unknown coefficients to be determined. They can be obtained by solving the linear system of equations of the form

$$\begin{aligned} \sum_{k=1}^{Ni} \alpha_k \varphi_k(X_i, Y_i) + \sum_{j=1}^L \beta_j p_j(X_i, Y_i) &= \tilde{b}^{(\text{iter}-1)}(X_i, Y_i), \quad i = 1, 2, \dots, Ni, \\ \sum_{j=1}^{Ni} \alpha_j p_k(X_j, Y_j) &= 0, \quad k = 1, 2, \dots, L. \end{aligned} \quad (32)$$

When the constants α_k and β_j are computed, the approximate particular solution $\Psi_p^{(\text{iter})}(X, Y)$ is of the following form:

$$\Psi_p^{(\text{iter})}(X, Y) \approx \sum_{k=1}^{Ni} \alpha_k \psi_k(X, Y) + \sum_{j=1}^L \beta_j q_j(X, Y), \quad (33)$$

where ψ_k and q_j are the particular solutions corresponding to the functions φ_k and p_j , respectively. Note that they are associated with the operator ∇^4 of the governing equation such that the following equations are satisfied $\nabla^4 \psi_k(X, Y) = \varphi_k(X, Y)$ and $\nabla^4 q_j(X, Y) = p_j(X, Y)$ (for details see, e.g., [Chen et al. 2014; Jankowska and Kołodziej 2015]).

Step 2-4-2. Compute the general solution.

The general solution $\Psi_h^{(\text{iter})}(X, Y)$ satisfies the homogeneous governing equation of the form $\nabla^4 \Psi_h^{(\text{iter})}(X, Y) = 0$ with the modified boundary conditions

$$\begin{aligned} G_{1l}(\Psi_h^{(\text{iter})}(X, Y)) &= g_{1l}(X, Y) - G_{1l}(\Psi_p^{(\text{iter})}(X, Y)), \\ G_{2l}(\Psi_h^{(\text{iter})}(X, Y)) &= g_{2l}(X, Y) - G_{2l}(\Psi_p^{(\text{iter})}(X, Y)), \end{aligned} \quad (34)$$

for $l = 1, 2, \dots, Nl$. The above boundary value problem can be solved with the MFS. The approximate general solution is of the form

$$\Psi_h^{(\text{iter})}(X, Y) \approx \sum_{i=1}^{Ns} c_i \phi_{1i}(X, Y) + \sum_{i=1}^{Ns} d_i \phi_{2i}(X, Y), \quad (35)$$

where the unknown values of coefficients c_i , d_i , $i = 1, 2, \dots, Ns$, present in (35), can be obtained, if we solve a linear system of collocation equations (compare Step 2 of the Algorithm 1).

Step 2-5. Since the solution $\Psi^{(\text{iter})}$ is known, compute $\tilde{\sigma}_{\text{eq},m}^{(\text{iter})}$ (the equation (24)) at all discretization points.

Note that Steps 2-2 to 2-4 describe how to compute the approximate solution of the inhomogeneous boundary-value equation (15)–(16) based on the plastic strain increments obtained in the previous iteration step. The successive approximations of the plastic strain increments can be found with the approach proposed in [Mendelson 1968] in the following way.

Step 2-6. Compute a new distribution of the plastic strain increments at all discretization points.

For all discretization points such that $\tilde{\sigma}_{\text{eq},m}^{(\text{iter}-1)} > 1$, apply a method presented in a block diagram (see Figure 4). This approach uses the stresses σ_{XX} , σ_{YY} , σ_{XY} obtained with the solution $\Psi^{(\text{iter})}$ together with the equivalent plastic strain increment $\Delta\tilde{\varepsilon}_{\text{eq}}^{p(\text{iter}-1)}$ (the equation (25)) and the corresponding equivalent stress $\tilde{\sigma}_{\text{eq}}^{(\text{iter}-1)}$ determined from the stress-strain curve (see Figure 5) to find a new distribution $\Delta\varepsilon_{XX}^{p(\text{iter})}$, $\Delta\varepsilon_{YY}^{p(\text{iter})}$, $\Delta\varepsilon_{XY}^{p(\text{iter})}$ of the plastic strain increments with the Prandtl–Reuss relations (23).

For the remaining discretization points, take $\Delta\varepsilon_{XX}^{p(\text{iter})} = \Delta\varepsilon_{YY}^{p(\text{iter})} = \Delta\varepsilon_{XY}^{p(\text{iter})} = 0$.

Step 2-7. Take two successive distributions of the plastic strain increments to compute the maximum distance d between two approximate solutions and the root mean square error $\delta^{(\text{iter})}$ of the boundary conditions fulfillment at Nt test points located on the boundary at each iteration step, i.e.,

$$d = \max\{d_{XX}, d_{YY}, d_{XY}\}, \quad \delta^{(\text{iter})} = \sqrt{\sum_{i=1}^{Nt} [\sigma_b(X_i, Y_i) - \sigma_a^{(\text{iter})}(X_i, Y_i)]^2 / Nt}, \quad (36)$$

where

$$d_{ij} = \sqrt{\sum_{k=1}^{Ni} [\Delta\varepsilon_{ij}^{p(\text{iter})}(X_k, Y_k) - \Delta\varepsilon_{ij}^{p(\text{iter}-1)}(X_k, Y_k)]^2 / Ni}. \quad (37)$$

σ_b denotes an exact value of the stress at a given test point on the boundary and σ_a represents the approximate value of the stress computed with the method proposed. Choose a tolerance value TOL. If $d \leq \text{TOL}$ and the root mean square error $\delta^{(\text{iter})}$ provides a sufficient accuracy of the result, then stop the internal iteration process and go further to Step 1-3. Else, take $\text{iter} = \text{iter} + 1$ and go back to Step 2-2.

Note that if the distance d is increasing for successive iterations, then the iteration process is not convergent and it is stopped. Similarly as in the case when the maximum number of iterations is exceeded before the accuracy is achieved.

Step 1-3. Take $m = m + 1$, go back to Step 1-2 and continue the main iteration process.

Finite difference approximation of partial derivatives. We can approximate values of all partial derivatives of the plastic strain increments that are needed in (19) for the function $\Delta\tilde{g}(X, Y)$ with the finite difference formulas (see, e.g., [Anderson et al. 1984; Orkisz 1998; Li and Wang 2003]). Then, values of the partial derivatives of the accumulated plastic strains that are required in (18) for the function $\tilde{g}(X, Y)$ can be easily obtained. The simplest method assumes the differentiation of the equations (20) and then the computation of the sums of the appropriate partial derivatives of the plastic strain increments. Note that values of the partial derivatives present in (19) are computed for the plastic strain increments corresponding to the interpolation points but for the appropriate finite difference equations we take the plastic strain increments that correspond to the discretization points. Such an approach increases an accuracy of the finite difference approximation. That is why, throughout the Algorithm 2, we compute values of the plastic strain increments at all discretization points.

The discretization points used in finite difference formulas are presented in Figures 3 and 6. We denote by O a given interpolation point. Furthermore, A_1, A_2, A_3 and B_1, B_2, B_3 represent the neighboring discretization points lying on the same line as the point O along the x -axis. Similarly, C_1, C_2, C_3 and D_1, D_2, D_3 are the neighboring discretization points lying along the y -axis. We can also distinguish another set of uniformly distributed discretization points E, F, G, H (see Figure 6, left). The distance between two points along the x -axis is equal to h and the distance between two points along the y -axis is represented by k . Subsequently, we refer to these distances as mesh increments.

Let P stands for any interpolation or discretization point considered. Subsequently, we denote by u_P a value of the appropriate increment of plastic strains $\Delta\varepsilon_{XX}^P$, $\Delta\varepsilon_{YY}^P$ or $\Delta\varepsilon_{XY}^P$ at the point P , respectively. For the great majority of the interpolation points, values of the appropriate partial derivatives can be approximated with the central finite difference formulas (see also Figure 6, left) given as

$$\frac{\partial^2 u_O}{\partial x^2} \approx \frac{u_{B1} - 2u_O + u_{A1}}{h^2}, \quad \frac{\partial^2 u_O}{\partial y^2} \approx \frac{u_{D1} - 2u_O + u_{C1}}{k^2}, \quad \frac{\partial^2 u_O}{\partial x \partial y} \approx \frac{u_E - u_F - u_G + u_H}{4hk}. \quad (38)$$

Nevertheless, since the plate is of irregular domain, then for some selected interpolation points located near the boundary, we have to use special formulas for the finite difference approximation. These formulas take into account different mesh increments. Such a general case is presented in Figure 6, right. As we can see, for given values of h and k , the distances between some neighboring points along the x and y axes can be smaller. In general, they can be determined by the coefficients (positive and less or equal to 1) denoted and defined as $\alpha_1 = |A_1 O|/h$, $\beta_1 = |B_1 O|/h$, $\gamma_1 = |C_1 O|/k$ and $\eta_1 = |D_1 O|/k$ (see Figure 6, right), respectively.

A choice of the appropriate finite difference formula depends on a position of the interpolation point with respect to the boundary. In most cases, each interpolation point has all their neighboring discretization points, i.e., $A_1, B_1, C_1, D_1, E, F, G, H$, even if some mesh increments are smaller than h and k . Then, we can use the following central finite difference formulas:

$$\frac{\partial^2 u_O}{\partial x^2} \approx \frac{2(\alpha_1 u_{B1} - (\alpha_1 + \beta_1)u_O + \beta_1 u_{A1})}{\alpha_1 \beta_1 (\alpha_1 + \beta_1) h^2}, \quad \frac{\partial^2 u_O}{\partial y^2} \approx \frac{2(\gamma_1 u_{D1} - (\gamma_1 + \eta_1)u_O + \eta_1 u_{C1})}{\gamma_1 \eta_1 (\gamma_1 + \eta_1) k^2}, \quad (39)$$

$$\frac{\partial^2 u_O}{\partial x \partial y} \approx \frac{1}{2h} \left(\frac{\partial u_{B1}}{\partial y} - \frac{\partial u_{A1}}{\partial y} \right). \quad (40)$$

Note that values of the partial derivatives of the first order present in (40) can be approximated with the central finite difference formula (41)₁, where P denotes a given discretization point (e.g., A_1, B_1 in (40)) and the notation $|_P$ indicates that the appropriate value is chosen with respect to the point P . We have

$$\frac{\partial u_P}{\partial y} \approx \frac{u_{D1}|_P - u_{C1}|_P}{(\gamma_1|_P + \eta_1|_P)k}, \quad \frac{\partial u_P}{\partial y} \approx \frac{3u_P - 4u_{C1}|_P + u_{C2}|_P}{2k}, \quad \frac{\partial u_P}{\partial y} \approx \frac{-3u_P + 4u_{D1}|_P - u_{D2}|_P}{2k}. \quad (41)$$

Finally, we consider the case when a given interpolation point (located very close to the boundary of the narrowed region) does not have some of its neighboring discretization points. We deal with such a situation rarely. If a number of uniformly distributed interpolation points is large, then a distance between a given interpolation point and some corresponding (located on the boundary) discretization point that should be also considered is equal or close to zero (see Section 3 and Figure 3). In such a case we do not include this point in the set of all discretization points used for further computations. Hence, for the

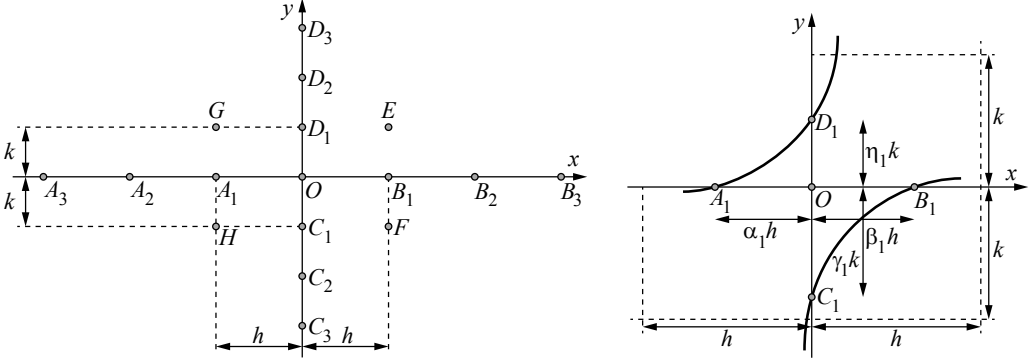


Figure 6. The distribution of the discretization points used in the finite difference formulas.

approximation of the second order derivatives with respect to x and y , we can use the backward (42)₁, (43)₁ or forward (42)₂, (43)₂ finite difference formulas given as follows:

$$\frac{\partial^2 u_O}{\partial x^2} \approx \frac{2u_O - 5u_{A_1} + 4u_{A_2} - u_{A_3}}{h^2}, \quad \frac{\partial^2 u_O}{\partial x^2} \approx \frac{2u_O - 5u_{B_1} + 4u_{B_2} - u_{B_3}}{h^2}, \quad (42)$$

$$\frac{\partial^2 u_O}{\partial y^2} \approx \frac{2u_O - 5u_{C_1} + 4u_{C_2} - u_{C_3}}{k^2}, \quad \frac{\partial^2 u_O}{\partial y^2} \approx \frac{2u_O - 5u_{D_1} + 4u_{D_2} - u_{D_3}}{k^2}. \quad (43)$$

Similarly, in the case of the mixed second order partial derivative, we can apply the following backward (44)₁ or forward (44)₂ finite differences:

$$\frac{\partial^2 u_O}{\partial x \partial y} \approx \frac{1}{2h} \left(3 \frac{\partial u_O}{\partial y} - 4 \frac{\partial u_{A_1}}{\partial y} + \frac{\partial u_{A_2}}{\partial y} \right), \quad \frac{\partial^2 u_O}{\partial x \partial y} \approx \frac{1}{2h} \left(-3 \frac{\partial u_O}{\partial y} + 4 \frac{\partial u_{B_1}}{\partial y} - \frac{\partial u_{B_2}}{\partial y} \right). \quad (44)$$

Depending on the existence and the location of the neighboring discretization points, for the approximation of the first order partial derivatives present in (44) we can choose the appropriate formula from (41).

Note that for the approximation of the partial derivatives proposed above, we take the finite difference formulas of the second order. The only exception are the finite differences (39) and (41)₁. They are of the first order accuracy due to the mesh increments that are smaller than h and k . However, for $\alpha_1 = \beta_1 = 1$ in (39)₁ and $\gamma_1 = \eta_1 = 1$ in (39)₂, the appropriate finite difference formulas reduce to the forms (38)₁ and (38)₂ of the second order accuracy, respectively. Similarly, the equation (41)₁ becomes for $\gamma_1 = \eta_1 = 1$ the central finite difference of the second order.

4. Numerical experiments

For the problem considered we choose the plate with two different depths of the narrowing. We refer to them as: 1-A (if $a = 1$, $b = 0.5$) and 1-B (if $a = 1$, $b = 0.25$), respectively. We choose $n = 0.5$ for the parameter of the elastic-plastic model (1) and we take the following material parameters: $E = 2 \times 10^{11}$ [Pa], $\nu = 0.3$, $\sigma_0 = 2 \times 10^8$ [Pa], $\varepsilon_0 = 1 \times 10^{-3}$. Further, for these two boundary-value problems we choose the loading paths to the state of stress $\tilde{\sigma}_B$. The algorithm proposed in Section 3 produces a sequence of results for each successive value of $\tilde{\sigma}_{B_m}$, if the appropriate step size is chosen as $h_{\tilde{\sigma}_B} = \tilde{\sigma}_{B_m} - \tilde{\sigma}_{B_{m-1}} = 0.0125$. The first interpolation points such that the plastic deformation occurs can be detected for $\tilde{\sigma}_B = 0.6375$ in the case of the geometry 1-A and $\tilde{\sigma}_B = 0.475$ in the case of the geometry 1-B.

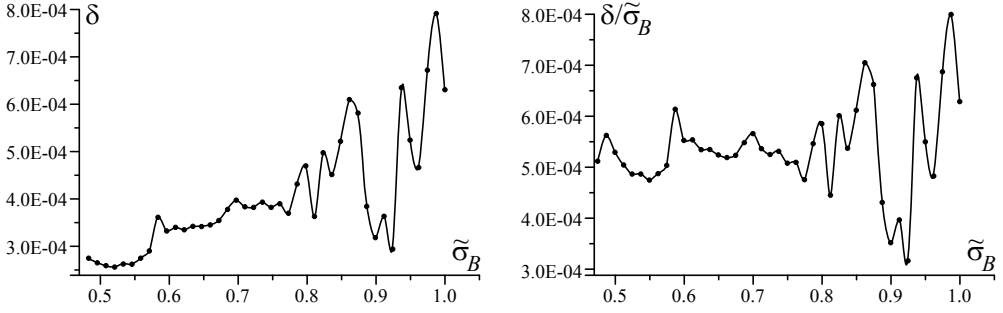


Figure 7. The root mean square error (left) and the root mean square error normalized with $\tilde{\sigma}_B$ (right) of the boundary conditions fulfillment obtained for the plate of the geometry 1-B after a constant number of eight iteration steps.

The parameters of the meshless methods were chosen so that the acceptable and small root mean square error of the solution could be achieved. Subsequently, we denote by Mc , Ms and Mi the number of collocation, source and interpolation points located on the shorter side of the plate (e.g., AB or CD). Furthermore, iMd is the number of additional intermediate discretization points placed between each two interpolation points (see Figure 3). We have $Mi = 11$, $iMd = 4$, $s = 0.2$ and $c = 0.1$. We also take $Mc = 80$, $Ms = 80$ for the geometry 1-A and $Mc = 60$, $Ms = 60$ for the geometry 1-B, respectively. For these values of parameters the distance between two neighboring interpolation points along the x and y axes is equal to 4.1667×10^{-2} and the mesh increments for the finite difference approximation are given by $h = k = 8.3333 \times 10^{-3}$.

The optimal computational procedure preferred by the authors assumes that the number of iteration steps required to obtain the solution related to succeeding stresses $\tilde{\sigma}_{Bk}$ is chosen so that the root mean

Geometry	1-A	1-B
Side of plate / Boundary condition	δ	δ
$(\Gamma_{AB}, \Gamma_{DC}) \Psi_{YY} = \tilde{\sigma}_B$	6.220×10^{-4}	3.601×10^{-4}
$(\Gamma_{E_1B}, \Gamma_{E_2C}, \Gamma_{F_1A}, \Gamma_{F_2D}) \Psi_{XX} = 0$	2.777×10^{-3}	7.253×10^{-4}
$(\Gamma_{AB}, \Gamma_{DC}, \Gamma_{E_1B}, \Gamma_{E_2C}, \Gamma_{F_1A}, \Gamma_{F_2D}) \Psi_{XY} = 0$	2.287×10^{-3}	2.174×10^{-4}
$(\Gamma_{E_1E_2}) \Psi_{YY}n_x - \Psi_{XY}n_y = 0$	4.020×10^{-3}	2.880×10^{-4}
$(\Gamma_{E_1E_2}) \Psi_{XX}n_y - \Psi_{XY}n_x = 0$	1.637×10^{-3}	6.977×10^{-4}
$(\Gamma_{F_1F_2}) \Psi_{YY}n_x - \Psi_{XY}n_y = 0$	4.019×10^{-3}	2.880×10^{-4}
$(\Gamma_{F_1F_2}) \Psi_{XX}n_y - \Psi_{XY}n_x = 0$	1.636×10^{-3}	6.977×10^{-4}
(Γ) Total	2.496×10^{-3}	4.691×10^{-4}
Final distance d	4.825×10^{-4}	4.018×10^{-3}

Table 1. Values of the root mean square error δ of the boundary conditions fulfillment for the different boundary conditions corresponding to the appropriate sides of the plate, the final distance d between to two last successive distributions of the plastic strain increments obtained with the algorithm proposed for $\tilde{\sigma}_B = 0.8$ and the geometries 1-A and 1-B. Eight iterations in total were used in each case.

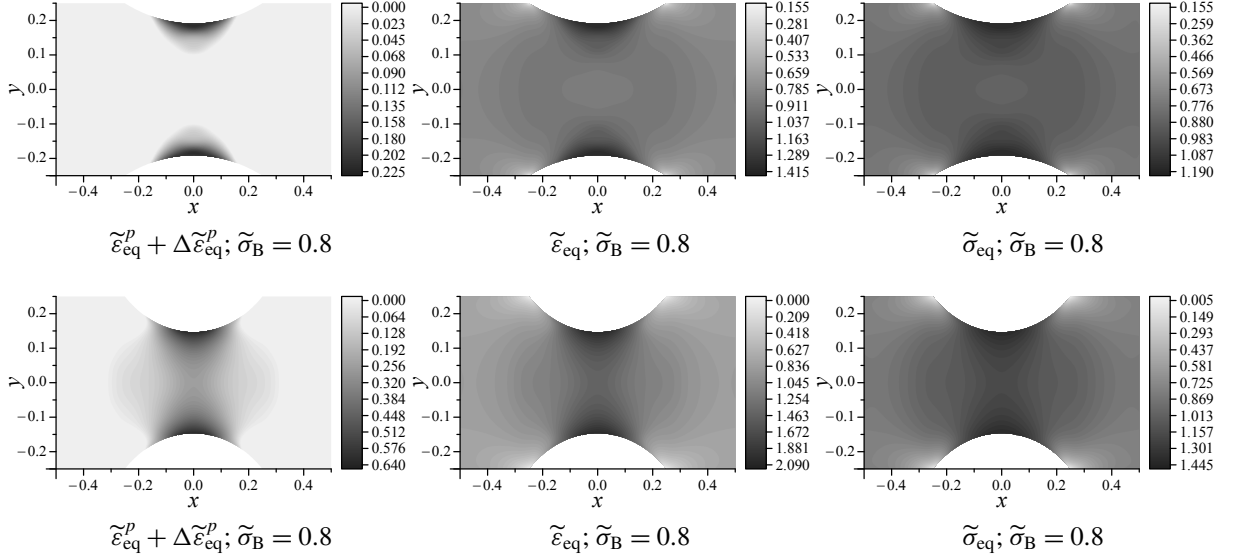


Figure 8. The comparison of the equivalent plastic strains $\tilde{\varepsilon}_{\text{eq}}^p + \Delta\tilde{\varepsilon}_{\text{eq}}^p$ (left), the equivalent total strains $\tilde{\varepsilon}_{\text{eq}}$ (middle) and the equivalent stress $\tilde{\sigma}_{\text{eq}}$ (right) in the plate of the geometry 1-A (top) and 1-B (bottom), respectively.

square error and a given tolerance imposed on the iteration process are sufficiently small. Nevertheless, since the accuracy of the solution is acceptable also for the constant number of iterations, we always perform eight iteration steps. Note that all computations were performed with the C++ libraries for the floating-point conversions in the double extended precision format (dedicated for the Intel C++ compiler) as proposed in [Jankowska 2010].

First, we present the accuracy of the approximate solution obtained for different conditions of loading for the plate of the geometry 1-B. As we can see in Figure 7, the root mean square error and the normalized root mean square error of the boundary conditions fulfillment obtained after a constant number of 8 iteration steps remain of the same order. The curve profiles indicate however that for larger values of the stress $\tilde{\sigma}_B$ more iteration steps (or just their different numbers) are required to retain the assumed accuracy.

In Table 1 we can see a comparison of values of the root mean square error of the boundary conditions fulfillment for the different boundary conditions corresponding to the appropriate sides of the plate and the final distance between two last successive distributions of the plastic strain increments. Such results are provided for the loading state related to $\tilde{\sigma}_B = 0.8$ and both geometries 1-A and 1-B. Then, the appropriate distributions of the equivalent plastic strains, the equivalent total strains and the equivalent stress in the plate obtained for the same value of $\tilde{\sigma}_B = 0.8$ and both geometries are presented in Figure 8. The regions of elastic and plastic deformation can be observed there.

5. Conclusions

A method for solving some plane elastoplastic boundary-value problem describing the stress state in the plate subjected to uniaxial extension is proposed. It is based on the successive-approximation iteration

process that is further combined with the meshless methods (the method of fundamental solutions and the method of particular solutions). Due to the special form of the right-hand side function of the governing equation the approximation of some partial derivatives with finite difference formulas is also applied. The authors introduce a new set of auxiliary discretization points that is utilized to control the finite difference approximation accuracy. Such points are not directly used for solving a sequence of nonhomogeneous boundary-value problems involved. Hence, the dimensions of some linear systems of equations that appear in each iteration step due to the meshless methods applied, are as always limited to the number of collocation and interpolations points. Note that the discretization points are uniformly located in the domain (except for the ones that are placed in the neighborhood of the narrowing). However, there is an increasing number of papers that propose an application of irregular grid (cloud) of points for the finite difference approximation (see the generalized finite difference (GFD) methods proposed, e.g., in [Orkisz 1998; Benito et al. 2007]). On the other hand, an application of the meshless methods for the problem considered is easy even in the case of complicated geometries. Furthermore, since the solution, i.e., the stress function, is approximated by linear combinations of fundamental solutions and particular solutions, we can compute values of stresses and strains not only in the interpolation or discretization points but at any point in the domain.

In the opinion of the authors the meshless methods are good alternative to the mesh methods in the case of many scientific problems. So far they were mainly used for solving some linear initial-boundary value problems with the Picard iteration process or the Newton–Raphson method as possible algorithms for nonlinear problems. Recently, several efficient algorithms that can be used together with the meshless methods for solving the nonlinear problems, appeared in the literature. Some of them are based on perturbation techniques that transform a nonlinear problem into a sequence of linear problems (see, e.g., the homotopy analysis method (HAM) described in [Liao 2004; Tsai 2012] and the asymptotic numerical method (ANM) proposed in [Tri et al. 2012]). Furthermore, we can use the Kansa method [1990] by an approximation of a solution with a linear combination of radial basis functions. Such an approach results in a nonlinear system of equations to be solved.

References

- [Al-Gahtani 2012] H. J. Al-Gahtani, “DRM-MFS for two-dimensional finite elasticity”, *Eng. Anal. Bound. Elem.* **36**:10 (2012), 1473–1477.
- [Anderson et al. 1984] D. A. Anderson, J. C. Tannehill, and R. H. Pletcher, *Computational fluid mechanics and heat transfer*, Hemisphere Publishing, Washington, DC, 1984.
- [Balakrishnan and Ramachandran 1999] K. Balakrishnan and P. A. Ramachandran, “A particular solution Trefftz method for non-linear Poisson problems in heat and mass transfer”, *J. Comput. Phys.* **150**:1 (1999), 239–267.
- [Balakrishnan and Ramachandran 2001] K. Balakrishnan and P. A. Ramachandran, “Osculatory interpolation in the method of fundamental solution for nonlinear Poisson problems”, *J. Comput. Phys.* **172**:1 (2001), 1–18.
- [Balakrishnan et al. 2002] K. Balakrishnan, R. Sureshkumar, and P. A. Ramachandran, “An operator splitting–radial basis function method for the solution of transient nonlinear Poisson problems”, *Comput. Math. Appl.* **43**:3-5 (2002), 289–304.
- [Belytschko et al. 2000] T. Belytschko, W. K. Liu, and B. Moran, *Nonlinear finite elements for continua and structures*, Wiley, Chichester, 2000.
- [Benito et al. 2007] J. J. Benito, F. Ureña, and L. Gavete, “Solving parabolic and hyperbolic equations by the generalized finite difference method”, *J. Comput. Appl. Math.* **209**:2 (2007), 208–233.

- [Berezhnoĭ and Paĭmushin 2011] D. V. Berezhnoĭ and V. N. Paĭmushin, “Two formulations of elastoplastic problems and the theoretical determination of the location of neck formation in samples under tension”, *J. Appl. Math. Mech.* **75**:4 (2011), 447–462.
- [Bilotta and Casciaro 2007] A. Bilotta and R. Casciaro, “A high-performance element for the analysis of 2D elastoplastic continua”, *Comput. Methods Appl. Mech. Eng.* **196**:4-6 (2007), 818–828.
- [Boudaia et al. 2009] E. Boudaia, L. Bousshine, H. F. Fihri, and G. D. Saxce, “Modelling of orthogonal cutting by incremental elastoplastic analysis and meshless method”, *C. R. Méc.* **337**:11-12 (2009), 761–767.
- [Boumaiza and Aour 2014] D. Boumaiza and B. Aour, “On the efficiency of the iterative coupling FEM-BEM for solving the elasto-plastic problems”, *Eng. Struct.* **72**:1 (2014), 12–25.
- [Burgess and Mahajerin 1987] G. Burgess and E. Mahajerin, “The fundamental collocation method applied to the nonlinear Poisson equation in two dimensions”, *Comput. Struct.* **27**:6 (1987), 763–767.
- [Chakrabarty 1987] J. Chakrabarty, *Theory of plasticity*, McGraw-Hill, New York, 1987.
- [Chen 1995] C. S. Chen, “The method of fundamental solutions for non-linear thermal explosions”, *Commun. Numer. Methods Eng.* **11**:8 (1995), 675–681.
- [Chen et al. 2014] W. Chen, Z.-J. Fu, and C. S. Chen, *Recent advances in radial basis function collocation methods*, Springer, Heidelberg, 2014.
- [Crisfield 1997] M. A. Crisfield, *Non-linear finite element analysis of solids and structures*, Wiley, Chichester, 1997.
- [Cui et al. 2009] X. Y. Cui, G. R. Liu, G. Y. Li, G. Y. Zhang, and G. Y. Sun, “Analysis of elastic-plastic problems using edge-based smoothed finite element method”, *Int. J. Press. Vessels Pip.* **86**:10 (2009), 711–718.
- [Dai et al. 2006] K. Y. Dai, G. R. Liu, X. Han, and Y. Li, “Inelastic analysis of 2D solids using a weak-form RPIM based on deformation theory”, *Comput. Methods Appl. Mech. Eng.* **195**:33-36 (2006), 4179–4193.
- [Deng et al. 2011] Q. Deng, C. Li, S. Wang, H. Zheng, and X. Ge, “A nonlinear complementarity approach for elastoplastic problems by BEM without internal cells”, *Eng. Anal. Bound. Elem.* **35**:3 (2011), 313–318.
- [Dong and Bonnet 1998] C. Y. Dong and M. Bonnet, “Symmetric-iterative solution of coupled BE and FE discretizations for elastoplastics”, *Comput. Methods Appl. Mech. Eng.* **178**:1-2 (1998), 171–182.
- [Fairweather and Karageorghis 1998] G. Fairweather and A. Karageorghis, “The method of fundamental solutions for elliptic boundary value problems”, *Adv. Comput. Math.* **9**:1-2 (1998), 69–95.
- [Fairweather et al. 2003] G. Fairweather, A. Karageorghis, and P. A. Martin, “The method of fundamental solutions for scattering and radiation problems”, *Eng. Anal. Bound. Elem.* **27**:7 (2003), 759–769.
- [Fallahi and Hosami 2011] M. Fallahi and M. Hosami, “The quasi-linear method of fundamental solution applied to transient non-linear Poisson problems”, *Eng. Anal. Bound. Elem.* **35**:3 (2011), 550–554.
- [Feng et al. 2013] P. Y. Feng, N. Ma, and X. C. Gu, “Application of method of fundamental solutions in solving potential flow problems for ship motion prediction”, *J. Shanghai Jiaotong Univ. Sci.* **18**:2 (2013), 153–158.
- [Gao and Davies 2000] X. W. Gao and T. G. Davies, “An effective boundary element algorithm for 2D and 3D elastoplastic problems”, *Int. J. Solids Struct.* **37**:36 (2000), 4987–5008.
- [Jankowska 2010] M. A. Jankowska, “Remarks on algorithms implemented in some C++ libraries for floating-point conversions and interval arithmetic”, pp. 436–445 in *Parallel processing and applied mathematics*, edited by R. Wyrzykowski et al., Lecture Notes in Computer Science **6068**, Springer, Berlin, 2010.
- [Jankowska and Kołodziej 2013] M. A. Jankowska and J. A. Kołodziej, “The method of fundamental solutions together with the successive-approximation method as an alternative approach to solving some plane elastoplastic problem”, pp. 1 in *COM-PLAS 2013 - XII International Conference on Computational Plasticity* (Barcelona, Spain, 2013), edited by E. Onate et al., International Center for Numerical Methods in Engineering (CIMNE), Barcelona, Spain, 2013.
- [Jankowska and Kołodziej 2014] M. A. Jankowska and J. A. Kołodziej, “Application of the method of fundamental solutions for the study of the stress state of the plate subjected to uniaxial tension”, pp. 20–22 in *TRECOP 2014 - International Symposium on Trends in Continuum Physics* (Bedlewo, 2014), edited by B. T. Maruszewski et al., Agencja Reklamowa COMPRINT, Poznan, Poland, 2014.

- [Jankowska and Kołodziej 2015] M. A. Jankowska and J. A. Kołodziej, “On the application of the method of fundamental solutions for the study of the stress state of a plate subjected to elastic–plastic deformation”, *Int. J. Solids Struct.* **67–68** (2015), 139–150.
- [Kansa 1990] E. J. Kansa, “Multiquadrics—a scattered data approximation scheme with applications to computational fluid-dynamics, I: Surface approximations and partial derivative estimates”, *Comput. Math. Appl.* **19**:8-9 (1990), 127–145.
- [Karageorghis and Fairweather 1989] A. Karageorghis and G. Fairweather, “The method of fundamental solutions for the solution of nonlinear plane potential problems”, *IMA J. Numer. Anal.* **9**:2 (1989), 231–242.
- [Karageorghis and Lesnic 2008] A. Karageorghis and D. Lesnic, “Steady-state nonlinear heat conduction in composite materials using the method of fundamental solutions”, *Comput. Methods Appl. Mech. Eng.* **197**:33-40 (2008), 3122–3137.
- [Karageorghis et al. 2011] A. Karageorghis, D. Lesnic, and L. Marin, “A survey of applications of the MFS to inverse problems”, *Inverse Probl. Sci. Eng.* **19**:3 (2011), 309–336.
- [Kojić and Bathe 2005] M. Kojić and K.-J. Bathe, *Inelastic analysis of solids and structures*, Springer, Berlin, 2005.
- [Kołodziej et al. 2013] J. A. Kołodziej, M. A. Jankowska, and M. Mierzwiczak, “Meshless methods for the inverse problem related to the determination of elastoplastic properties from the torsional experiment”, *Int. J. Solids Struct.* **50**:25-26 (2013), 4217–4225.
- [Li and Wang 2003] Z. Li and C. Wang, “A fast finite difference method for solving Navier–Stokes equations on irregular domains”, *Commun. Math. Sci.* **1**:1 (2003), 180–196.
- [Li and Zhu 2009] X. Li and J. Zhu, “The method of fundamental solutions for nonlinear elliptic problems”, *Eng. Anal. Bound. Elem.* **33**:3 (2009), 322–329.
- [Li et al. 2014] M. Li, C. S. Chen, C. C. Chu, and D. L. Young, “Transient 3D heat conduction in functionally graded materials by the method of fundamental solutions”, *Eng. Anal. Bound. Elem.* **45** (2014), 62–67.
- [Liao 2004] S. Liao, *Beyond perturbation: Introduction to the homotopy analysis method*, CRC Series: Modern Mechanics and Mathematics **2**, Chapman & Hall/CRC, Boca Raton, FL, 2004.
- [Liu 2003] G. R. Liu, *Mesh free methods: Moving beyond the finite element method*, CRC Press, Boca Raton, FL, 2003.
- [Liu et al. 2011] H. Liu, Z. Xing, Z. Sun, and J. Bao, “Adaptive multiple scale meshless simulation on springback analysis in sheet metal forming”, *Eng. Anal. Bound. Elem.* **35**:3 (2011), 436–451.
- [Liu et al. 2012] Y. Liu, C. Wang, and Q. Yang, “Stability analysis of soil slope based on deformation reinforcement theory”, *Finite Elem. Anal. Des.* **58** (2012), 10–19.
- [Liu et al. 2013] X. Liu, M. A. Bradford, and R. E. Erkmén, “Non-linear inelastic analysis of steel–concrete composite beams curved in-plan”, *Eng. Struct.* **57** (2013), 484–492.
- [Marin and Lesnic 2007] L. Marin and D. Lesnic, “The method of fundamental solutions for nonlinear functionally graded materials”, *Int. J. Solids Struct.* **44**:21 (2007), 6878–6890.
- [Mendelson 1968] A. Mendelson, *Plasticity: Theory and application*, McMillan, New York, 1968.
- [Mollazadeh et al. 2011] M. Mollazadeh, M. J. Khanjani, and A. Tavakoli, “Applicability of the method of fundamental solutions to interaction of fully nonlinear water waves with a semi-infinite floating ice plate”, *Cold Regions Sci. Technol.* **69**:1 (2011), 52–58.
- [Ochiai 2011] Y. Ochiai, “Three-dimensional thermo-elastoplastic analysis by triple-reciprocity boundary element method”, *Eng. Anal. Bound. Elem.* **35**:3 (2011), 478–488.
- [Orkisz 1998] J. Orkisz, “Finite difference method, III”, pp. 336–432 in *Handbook of computational solid mechanics*, edited by M. Kleiber, Springer, Berlin, 1998.
- [Owen and Hinton 1980] D. R. J. Owen and E. Hinton, *Finite elements in plasticity: Theory and practice*, Pineridge Press, Swansea, 1980.
- [Oysu and Fenner 2006] C. Oysu and R. T. Fenner, “Coupled FEM-BEM for elastoplastic contact problems using lagrange multipliers”, *Appl. Math. Model.* **30**:3 (2006), 231–247.
- [Poza et al. 2009] L. P. Poza, F. Perazzo, and A. Angulo, “A meshless FPM model for solving nonlinear material problems with proportional loading based on deformation theory”, *Adv. Eng. Softw.* **40**:11 (2009), 1148–1154.

- [Shanazari and Fallahi 2010] K. Shanazari and M. Fallahi, “A quasi-linear technique applied to the method of fundamental solution”, *Eng. Anal. Bound. Elem.* **34**:4 (2010), 388–392.
- [Timoshenko and Goodier 1951] S. Timoshenko and J. N. Goodier, *Theory of elasticity*, 2nd ed., McGraw-Hill, New York, 1951.
- [Tri et al. 2011] A. Tri, H. Zahrouni, and M. Potier-Ferry, “Perturbation technique and method of fundamental solution to solve nonlinear Poisson problems”, *Eng. Anal. Bound. Elem.* **35**:3 (2011), 273–278.
- [Tri et al. 2012] A. Tri, H. Zahrouni, and M. Potier-Ferry, “High order continuation algorithm and meshless procedures to solve nonlinear Poisson problems”, *Eng. Anal. Bound. Elem.* **36**:11 (2012), 1705–1714.
- [Tsai 2012] C.-C. Tsai, “Homotopy method of fundamental solutions for solving certain nonlinear partial differential equations”, *Eng. Anal. Bound. Elem.* **36**:8 (2012), 1226–1234.
- [Uscilowska and Berendt 2013] A. Uscilowska and D. Berendt, “An implementation of the method of fundamental solutions for the dynamic response of von Karman nonlinear plate model”, *Int. J. Comput. Methods* **10**:2 (2013), 1341005.
- [Wang and Qin. 2006] H. Wang and Q. H. Qin., “A meshless method for generalized linear or nonlinear Poisson-type problems”, *Eng. Anal. Bound. Elem.* **30**:6 (2006), 515–521.
- [Wang and Qin. 2008] H. Wang and Q. H. Qin., “Meshless approach for thermo-mechanical analysis of functionally graded materials”, *Eng. Anal. Bound. Elem.* **32**:9 (2008), 704–712.
- [Wang et al. 2005] H. Wang, Q.-H. Qin., and Y. L. Kang, “A new meshless method for steady-state heat conduction problems in anisotropic and inhomogeneous media”, *Arch. Appl. Mech.* **74**:8 (2005), 563–579.
- [Wang et al. 2012] H. Wang, Q.-H. Qin, and X.-P. Liang, “Solving the nonlinear Poisson-type problems with F-Trefftz hybrid finite element model”, *Eng. Anal. Bound. Elem.* **36**:1 (2012), 39–46.
- [Yeon and Youn 2005] J.-H. Yeon and S. K. Youn, “Meshfree analysis of softening elastoplastic solids using variational multi-scale method”, *Int. J. Solids Struct.* **42**:14 (2005), 4030–4057.
- [Young et al. 2008] D. L. Young, C. M. Fan, S. P. Hu, and S. N. Atluri, “The Eulerian–Lagrangian method of fundamental solutions for two-dimensional unsteady Burgers’ equations”, *Eng. Anal. Bound. Elem.* **32**:5 (2008), 395–412.
- [Young et al. 2009] D. L. Young, Y. C. Lin, C. M. Fan, and C. L. Chiu, “The method of fundamental solutions for solving incompressible Navier–Stokes problems”, *Eng. Anal. Bound. Elem.* **33**:8-9 (2009), 1031–1044.

Received 2 Jan 2015. Revised 29 Jul 2015. Accepted 17 Aug 2015.

MALGORZATA A. JANKOWSKA: malgorzata.jankowska@put.poznan.pl

Institute of Applied Mechanics, Poznan University of Technology, Jana Pawła II 24, 60-965 Poznan, Poland

JAN ADAM KOŁODZIEJ: jan.kolodziej@put.poznan.pl

Institute of Applied Mechanics, Poznan University of Technology, Jana Pawła II 24, 60-965 Poznan, Poland

JOURNAL OF MECHANICS OF MATERIALS AND STRUCTURES

msp.org/jomms

Founded by Charles R. Steele and Marie-Louise Steele

EDITORIAL BOARD

ADAIR R. AGUIAR	University of São Paulo at São Carlos, Brazil
KATIA BERTOLDI	Harvard University, USA
DAVIDE BIGONI	University of Trento, Italy
YIBIN FU	Keele University, UK
IWONA JASIUK	University of Illinois at Urbana-Champaign, USA
C. W. LIM	City University of Hong Kong
THOMAS J. PENCE	Michigan State University, USA
DAVID STEIGMANN	University of California at Berkeley, USA

ADVISORY BOARD

J. P. CARTER	University of Sydney, Australia
D. H. HODGES	Georgia Institute of Technology, USA
J. HUTCHINSON	Harvard University, USA
D. PAMPLONA	Universidade Católica do Rio de Janeiro, Brazil
M. B. RUBIN	Technion, Haifa, Israel

PRODUCTION production@msp.org

SILVIO LEVY Scientific Editor


Cover photo: Ev Shafir

See msp.org/jomms for submission guidelines.

JoMMS (ISSN 1559-3959) at Mathematical Sciences Publishers, 798 Evans Hall #6840, c/o University of California, Berkeley, CA 94720-3840, is published in 10 issues a year. The subscription price for 2016 is US\$575/year for the electronic version, and \$735/year (+\$60, if shipping outside the US) for print and electronic. Subscriptions, requests for back issues, and changes of address should be sent to MSP.

JoMMS peer-review and production is managed by EditFLOW[®] from Mathematical Sciences Publishers.

PUBLISHED BY

 **mathematical sciences publishers**
nonprofit scientific publishing

<http://msp.org/>

© 2016 Mathematical Sciences Publishers

Special issue

Trends in Continuum Physics (TRECOP 2014)

Preface	BOGDAN T. MARUSZEWSKI, WOLFGANG MUSCHIK, ANDRZEJ RADOWICZ and KRZYSZTOF W. WOJCIECHOWSKI	1
Stress and displacement analysis of an auxetic quarter-plane under a concentrated force	PAWEŁ FRITZKOWSKI and HENRYK KAMIŃSKI	3
Laminar flow of a power-law fluid between corrugated plates	JAKUB KRZYSZTOF GRABSKI and JAN ADAM KOŁODZIEJ	23
A study of elastic-plastic deformation in the plate with the incremental theory and the meshless methods	MALGORZATA A. JANKOWSKA and JAN ADAM KOŁODZIEJ	41
Implementation of HAM and meshless method for torsion of functionally graded orthotropic bars	ANITA UŚCIEŁOWSKA and AGNIESZKA FRASKA	61
The application of the method of fundamental solutions in modeling auxetic materials	TOMASZ WALCZAK, GRAZYNA SYPNIEWSKA-KAMIŃSKA, BOGDAN T. MARUSZEWSKI and KRZYSZTOF W. WOJCIECHOWSKI	79